Proceedings of the 11th International IEEE
Conference on Intelligent Transportation Systems
Beijing, China, October 12-15, 2008

A UKF-NN Framework for System Identification of Small Unmanned Aerial Vehicles

Abhijit Kallapur, Mahendra Samal, Vishwas Puttige, Sreenatha Anavatti and Matthew Garratt

Abstract— **This paper presents a novel system identification framework for small unmanned aerial vehicles (UAVs) by combining an unscented Kalman filter (UKF) estimator with a neural network (NN) identifier. The method is effective for systems with low-cost, erroneous sensors where the sensor outputs cannot be used directly for system identification and control. The UKF state estimator computes error-compensated attitude and velocities by integrating sensor data from an inertial measurement unit (IMU) and a global positioning system (GPS). The NN identifier approximates the nonlinear dynamics of the UAV from the UKF estimated states, hence identifying the system. As an illustration, the UKF-NN system identification framework is applied to fixed-wing as well as rotary-wing 6-DOF multi-input-multi-output (MIMO) nonlinear UAV models.**

I. Introduction

Successful autonomous operation of unmanned aerial vehicles (UAVs) demands robust navigation, guidance and control (NGC) schemes. Neural Networks (NN) are a popular choice for identification and control of such vehicles [1], [2], [3]. Here, at UNSW@ADFA we have implemented an NN-based system identification in real-time for fixed-wing (Megasoar) [3] as well as rotary-wing (Eagle) [4] UAVs for flight control.

Flight control systems for UAVs are necessary to attain the commanded attitude and to maintain steady flight conditions when subjected to uncertainties. Robust control techniques capable of adapting to change in dynamics of the platform are necessary for autonomous flight. Such controllers can be developed with the aid of suitable system identification (ID) techniques. In order to implement control strategies in real-time we need accurate sensor information. With increasing emphasis on deployment of UAVs in urban environments, research is shifting towards developing smaller platforms with lighter payloads. A popular choice for low-cost, light-weight sensors are those belonging to the family of micro-electro-mechanical-sensors (MEMS). However, these sensors suffer with problems of drift and bias and hence cannot be used directly for UAV control. The need for intelligent sensor integration in order to compensate for sensor anomalies becomes a critical issue. Various forms of Kalman filters [5], [6], [7], [8], [9], [10] have been used for the process of sensor integration as long as the system dynamics are well defined. Depending upon the nonlinearities associated with the system we can either use an extended Kalman filter (EKF) or an unscented Kalman filter (UKF). Considering the advantages of UKF over EKF [7], [10], [11], [12] for highly nonlinear systems we shall use the UKF for UAV estimation. The UKF estimated, error-compensated sensor states can then be fed to the NN block for UAV identification and control. On these lines we propose a novel UKF-NN framework for system identification of small UAVs with limited payload capabilities. Among various sensors available we shall restrict our choice to two basic sensors, namely, the inertial measurement unit (IMU) and the global positioning system (GPS). It should be noted that Kalman filters have been used with NN with very little emphasis on the combination of UKF and NN. Moreover, the use of such filter-NN combinations have been restricted to NN training [13], [14], [15] as opposed to providing error-compensated sensor states and is the motivation for the proposed UKF-NN framework.

The remainder of this paper proceeds as follows: Section II defines the problem of system identification for small UAVs and introduces the proposed UKF-NN framework for identification. Section III describes a UKF estimator and provides UAV propagation and measurement dynamics. An insight into NNID for UAVs is presented in Section IV. The application of the proposed UKF-NN framework towards the system identification of a fixed-wing as well as a rotary-wing UAV are presented in Section V, followed by the conclusion and plans for future work in Section VI.

II. System Description

The design of flight control systems demands high-quality identification data that in turn need reliable sensor information. In order to provide error-compensated sensor states we propose a novel UKF-NN framework for the purpose of system identification of small UAVs. The UKF is used for sensor fusion whereas the NN identifies the system by approximating the nonlinear UAV dynamics from filter estimated states. A schematic of the UKF-NN identification system is as illustrated in Fig. 1.

In the proposed system, the servo inputs (δ) to the UAV plant are provided by the controller. The plant responds to servo deflections, which are then captured by the sensors onboard the UAV. Inaccuracies in sensor measurements may cause the aircraft to deviate from the desired trajectory by injecting erroneous data into the closed loop architecture. The UKF block is introduced to mitigate this problem by combining data from various sensors in order to estimate errors in them, hence providing suitable compensations. The servo deflections (δ) and sensor integration outputs ($\breve{y}$) are

The authors are with the School of Aerospace, Civil and Mechanical Engineering, University of New South Wales at the Australian Defence Force Academy, Canberra, ACT 2600, Australia {a.kallapur, m.samal, v.puttige, agsrenat, m.garratt}@adfa.edu.au

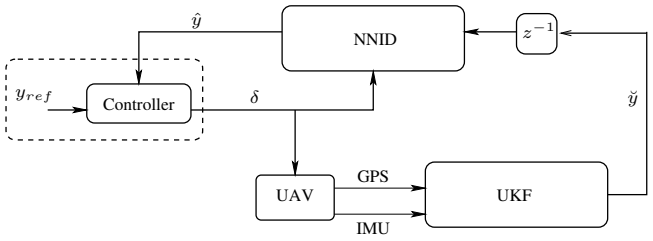

Fig. 1. UKF-NN framework for System Identification

fed to the NNID block. The NNID block based on the autoregressive exogenous (ARX) model identifies the system and predicts the future outputs ($\hat{y}$) based on their past and present values. The predicted outputs along with the commanded reference input (y_{ref}) are utilized by the controller block to generate the next set of servo deflections. An adaptive controller minimizes the error difference between the command reference and the NNID predictions. Since this paper emphasizes system identification, results from the controller will *not* be presented (hence the dotted lines around the controller block).

The UKF estimator and the NNID blocks are explained in sections III and IV respectively.

III. Unscented Kalman Filter Estimator

A. The Unscented Kalman Filter

The estimation of a coupled, nonlinear system with correlated noise is quite challenging in the design and implementation of NGC. EKF is a popular choice for this purpose but is known to diverge with increasing nonlinearities due to first order linearization of the nonlinear system [7], [11]. On the other hand, the UKF operates on the basis that *it is easier to approximate a Gaussian distribution than it is to approximate an arbitrary nonlinear function or transformation* [7], and has been accepted as a suitable estimation method.

Consider a nonlinear system described by,

$$\begin{aligned} \vec{x}_t &= \vec{f}(\vec{x}_{t-1}, \vec{u}_t, \vec{w}_t); \\ \vec{y}_t &= \vec{h}(\vec{x}_t, \vec{u}_t, \vec{v}_t) \end{aligned} \tag{1}$$

where $\vec{x}, \vec{u}, \vec{w}, \vec{v}$ are the states, inputs, process noise and measurement noise vectors in that order and $\vec{f}(\cdot)$ and $\vec{h}(\cdot)$ are nonlinear state and measurement functions respectively. For the system described in (1), the UKF can be applied as a recursive minimum mean square error (RMMSE) estimator where the state vector is augmented with noise vectors to form an augmented state vector:

$$\vec{x}_t^a = \left[\vec{x}_t^T \, \vec{w}_t^T \, \vec{v}_t^T\right]. \tag{2}$$

Various matrices and vectors for the UKF estimator can then be set as follows which can be recursively executed at each time step i.

- Initialize augmented states and covariances

$$\vec{x}_0^a = \left[\hat{\vec{x}}_0^T \, \vec{0} \, \vec{0}\right]^T;$$
$$\vec{P}_0^a = \begin{bmatrix} \vec{P}_0 & \vec{0} & \vec{0} \\ \vec{0} & \vec{Q} & \vec{0} \\ \vec{0} & \vec{0} & \vec{R} \end{bmatrix}.$$

- Computation of Sigma points ($\boldsymbol{\mathcal{X}}$) and weights (W) using Scaled Unscented Transform (SUT)

$$\boldsymbol{\mathcal{X}}_{t|t-1}^a = \left[\hat{\vec{x}}_{t-1}^a \;\; \left(\hat{\vec{x}}_{t-1}^a \pm \sqrt{(n_a + \lambda)\, \vec{P}_{t-1}^a}\right)\right];$$
$$W_i^{(m)} = W_i^{(c)} = 1/2(n_x + \lambda);$$
$$W_0^{(m)} = \lambda/(n_x + \lambda);$$
$$W_0^{(c)} = W_0^{(m)} + (1 - \alpha^2 + \beta).$$

- Time update

$$\boldsymbol{\mathcal{X}}_{t|t-1}^x = \vec{f}(\boldsymbol{\mathcal{X}}_{t-1}^x, \boldsymbol{\mathcal{X}}_{t-1}^w);$$
$$\hat{\vec{x}}_{t|t-1} = \sum_{i=0}^{2n_a} W_i^{(m)} \, \mathcal{X}_{i,t|t-1}^x;$$
$$\vec{P}_{t|t-1} = \sum_{i=0}^{2n_a} W_i^{(c)} \left[\mathcal{X}_{i,t|t-1}^x - \hat{\vec{x}}_{t|t-1}\right] \cdot \left[\mathcal{X}_{i,t|t-1}^x - \hat{\vec{x}}_{t|t-1}\right]^T;$$
$$\boldsymbol{\mathcal{Y}}_{t|t-1} = \vec{h}\left(\boldsymbol{\mathcal{X}}_{t|t-1}^x, \boldsymbol{\mathcal{X}}_{t-1}^v\right);$$
$$\hat{\vec{y}}_{t|t-1} = \sum_{i=0}^{2n_a} W_i^{(m)} \, \mathcal{Y}_{i,t|t-1}.$$

- Measurement update

$$\vec{P}_{\vec{y}_t \, \vec{y}_t} = \sum_{i=0}^{2n_a} W_i^{(c)} \left[\mathcal{Y}_{i,t|t-1} - \hat{\vec{y}}_{t|t-1}\right] \cdot \left[\mathcal{Y}_{i,t|t-1} - \hat{\vec{y}}_{t|t-1}\right]^T;$$
$$\vec{P}_{\vec{x}_t \, \vec{y}_t} = \sum_{i=0}^{2n_a} W_i^{(c)} \left[\mathcal{X}_{i,t|t-1} - \hat{\vec{x}}_{t|t-1}\right] \cdot \left[\mathcal{Y}_{i,t|t-1} - \hat{\vec{y}}_{t|t-1}\right]^T;$$
$$\vec{K}_t = \vec{P}_{\vec{x}_t \, \vec{y}_t} \, \vec{P}_{\vec{y}_t \, \vec{y}_t}^{-1};$$
$$\hat{\vec{x}}_t = \hat{\vec{x}}_{t|t-1} + \vec{K}_t(\vec{y}_t - \hat{\vec{y}}_{t|t-1});$$
$$\vec{P}_t = \vec{P}_{t|t-1} - \vec{K}_t \, \vec{P}_{\vec{y}_t \vec{y}_t} \, \vec{K}_t^T.$$

Here, $\boldsymbol{\mathcal{X}}^a = \left[(\boldsymbol{\mathcal{X}}^{\vec{x}})^T (\boldsymbol{\mathcal{X}}^{\vec{w}})^T (\boldsymbol{\mathcal{X}}^{\vec{v}})^T\right]$, λ is the composite scaling parameter, $n_a = n_x + n_w + n_v$, $\vec{P}$ represents covariance matrix, $\vec{Q}$ is the process noise matrix, $\vec{R}$ is the measurement noise matrix, $\vec{K}$ is the Kalman gain and $(\cdot)^{(m)}$ correspond to mean values whereas $(\cdot)^{(c)}$ correspond to covariance values. Further details about UKF and its implementation can be found in [7], [11], [16].

B. System Propagation and Measurement Equations

UKF was applied to a set of raw IMU data of angular rates and accelerations to estimate UAV attitude and body velocities at 20Hz. The same set of equations were used for both the fixed-wing as well as the rotary-wing models.

1) Process Model: The process model used for system propagation consists of nine coupled states described by [17],

$$\begin{aligned}
\dot{\phi} &= p + \tan\theta(q\sin\phi + r\cos\phi);\\
\dot{\theta} &= q\cos\phi - r\sin\phi;\\
\dot{\psi} &= \frac{q\sin\phi + r\cos\phi}{\cos\theta};\\
\dot{u} &= rv - qw - g^{'}\sin\theta + a_x;\\
\dot{v} &= pw - ru + g^{'}\sin\phi\cos\theta + a_y;\\
\dot{w} &= qu - pv + g^{'}\cos\phi\cos\theta + a_z;\\
\dot{\varepsilon_p} &= 0;\\
\dot{\varepsilon_q} &= 0;\\
\dot{\varepsilon_r} &= 0
\end{aligned} \tag{3}$$

where ϕ, θ, ψ represent attitude; u, v, w represent body velocities; p, q, r are the angular rates; a_x, a_y, a_z are body sensed accelerations and $\varepsilon_p, \varepsilon_q, \varepsilon_r$ are the gyro bias terms.

2) Measurement Model: The errors from INS time propagation in (3) are corrected using attitude measurements obtained from GPS and accelerometer accelerations and GPS measured velocities denoted by the measurement vector, $\vec{y} = [\tilde{\phi}\ \tilde{\theta}\ \tilde{\psi}\ \tilde{u}\ \tilde{v}\ \tilde{w}]^T$.

- *Attitude Measurement*
  The attitude estimation scheme adopted in this paper is derived from the implementation described in [9]. The basic idea is to correct for the attitude computed using an INS by acceleration information from both the accelerometers as well as the GPS. In the case of a non-accelerating UAV the local gravity vector $[0\ 0\ g]^T$ can be used as a reference frame to compute the roll and pitch angles as in (8). However, if the UAV is accelerating relative to the earth-centered-earth-fixed (ECEF) frame, the accelerometers onboard the vehicle will measure the apparent acceleration $[g - a_{uav}]$, where a_{uav} is the actual UAV acceleration [9]. In such cases GPS accelerations can be used as a reference to correct for attitude errors by solving (8) for roll and pitch angles using methods such as the principal component analysis (PCA). GPS measurements on the other hand provide a_{uav} that need to be rotated by the heading angle in order to align them with the UAV X and Y body axis so as to obtain a new reference vector. Considering $[a_{GPS_x}, a_{GPS_y}, a_{GPS_z}]$ to be GPS accelerations and $[a_x, a_y, a_z]$ to be the accelerometer outputs, the computed attitude measurements $(\tilde{\phi}, \tilde{\theta}, \tilde{\psi})$ are described as [9],
  - Heading measurements
  $$\tilde{\psi} = \tan^{-1}\left(\frac{V_y}{V_x}\right). \tag{4}$$
  - Reference vector
  $$\begin{aligned}
  r_x &= -(\cos(\tilde{\psi})\, a_{GPS_x} + \sin(\tilde{\psi})\, a_{GPS_y});\\
  r_y &= -(-\sin(\tilde{\psi})\, a_{GPS_x} + \cos(\tilde{\psi})\, a_{GPS_y});\\
  r_z &= g - a_{GPS_z}.
  \end{aligned} \tag{5}$$
  - Pitch measurement
  $$\begin{aligned}
  \delta_\theta &= \left(\frac{r_x a_x + r_z\sqrt{r_x^2 + r_z^2 - a_x^2}}{r_x^2 + r_z^2}\right);\\
  \tilde{\theta} &= \tan^{-1}\left(\frac{\delta_\theta r_x - a_x}{\delta_\theta r_z}\right).
  \end{aligned} \tag{6}$$
  - Roll measurement
  $$\begin{aligned}
  r_\theta &= \left(r_x\sin(\theta) + r_z\cos(\theta)\right);\\
  \delta_\phi &= \left(\frac{r_y a_y + r_\theta\sqrt{r_y^2 + r_\theta^2 - a_y^2}}{r_y^2 + r_\theta^2}\right);\\
  \tilde{\phi} &= \tan^{-1}\left(\frac{-\delta_\phi r_y + a_y}{\delta_\phi r_\theta}\right).
  \end{aligned} \tag{7}$$

- *Velocity Measurement*
  In order to measure body velocities the GPS measured ECEF velocities $[V_X\ V_y\ V_z]^T$ have to be transformed into body velocities $[\tilde{u}\ \tilde{v}\ \tilde{w}]^T$ using the rotation matrix $\vec{R}_{e->b}$ as:
  $$\begin{bmatrix}\tilde{u}\\ \tilde{v}\\ \tilde{w}\end{bmatrix} = \vec{R}_{e->b}\begin{bmatrix}V_X\\ V_Y\\ V_Z\end{bmatrix} \tag{8}$$
  with $\vec{R}_{e->b} = f(\phi, \theta, \psi)$.

The values of $\tilde{\phi}$, $\tilde{\theta}$, $\tilde{\psi}$, $\tilde{u}$, $\tilde{v}$, $\tilde{w}$ can then be used as measurement inputs to the UKF for robust sensor fusion.

IV. Neural Network Identification

In this paper, a recurrent NN with an ARX structure is considered for the UAV identification problem. In the ARX-NN model, the network retains information about the past dynamics to predict the next output. The predicted output of a nonlinear ARX model is given by [18], [19], [20],

$$\begin{aligned}
\widehat{y}(t) =& g(\omega, \Phi(t));\\
\omega =& (a_1, a_2, ...a_{na}, b_1, b_2, ..., b_{nb});\\
\Phi(t) =& (y(t-1), ...y(t-na), u(t), ..., u(t-nb))
\end{aligned} \tag{9}$$

where $g(\cdot)$ is a nonlinear function, Φ is the regressor vector available from memory and ω is the coefficient matrix which quantifies the influence of past outputs (y) and inputs (u) on each of the subsequent outputs. The coefficient matrix (ω) can be obtained from the mathematical model of the system. However, for a nonlinear system such as the UAV, an accurate mathematical model may not be available. As a solution, an approximate black-box model based on NN can be utilized. A two layered feed-forward NN is considered to

possess global approximation capabilities [21]. The output of a two layered neural network is given by,

$$\widehat{y}_i(t) = F_i(\sum_{j=1}^{l_1} W_{2ji} G_j(\sum_{k=1}^{l_2} W_{1kj} x_k(t) + W_{1k0}) + W_{2j0}) \tag{10}$$

where F_i and G_i are the activation functions; l_1 and l_2 are the number of neurons in the two layers; W_{1k0} and W_{2j0} are the bias to the two layers and x_k is the network input. W_{1kj} and W_{2ji} are the weights from the hidden and output layers respectively. These weights correspond to ω in (9).

Iterative training is performed to minimize the mean squared error (MSE) using the Levenberg-Marquardt (LM) technique. The goal of training is to obtain the most suitable weights in order to provide the least possible prediction error. The MSE is given by,

$$V_N(\omega) = \frac{1}{N} \sum_{t=1}^{N} (y(t) - \widehat{y}(t))^2. \tag{11}$$

The updated value for ω after each iteration is given by,

$$\omega_{i+1} = \omega_i - \mathbf{R}_i^{-1} \mathbf{G}_i \tag{12}$$

where $\mathbf{R}$ is a matrix responsible for the search direction and $\mathbf{G}$ is the gradient of the mean square error given by,

$$\mathbf{G}_i = V_N(\omega_i) = -\frac{2}{N} \sum_{t=1}^{N} (y(t) - \widehat{y}(t|\omega_i)) \psi(t, \omega_i) \tag{13}$$

with Ψ depicting the derivative of the predicted output with respect to the co-efficient matrix ω. The search direction is given by $\mathbf{R}_i^{-1}\mathbf{G}_i$ and is used to update the weights. For the LM method, $\mathbf{R}_i$ is given as

$$\mathbf{R}_i = \frac{1}{N} \sum_{t=1}^{N} (\Psi(t, \widehat{\omega_i}), \Psi^T(t, \widehat{\omega_i})) + \mu \mathbf{I} \tag{14}$$

V. Results

This section briefly describes the UAV simulation process and presents system identification results obtained by applying the UKF-NN framework.

A. Simulation Process

Matlab® Simulink® was used to generate models for both the fixed-wing as well as the rotary-wing UAVs. A brief description of the simulation models is given here.

1) Rotary-wing UAV Model: A Matlab® Simulink® model for a small unmanned Eagle helicopter was designed and programmed at UNSW@ADFA [22]. This model incorporates various servo dynamics and sensor characteristics to provide a desired match with experimental data. It is used as a virtual platform for the development of sensor data fusion algorithms and design of controllers. The simulation takes into account,

- nonlinear rigid body equations of motion;
- main rotor flap dynamics;
- Bell-Hiller stabilizer bar dynamics;
- approximate servo dynamics;
- fuselage and tailplane aerodynamic forces;
- sensor lag, filtering, offsets and noise;
- wind gust and turbulence effects.

The ground effect, interaction of rotor downwash with the fuselage and rotor lead-lag mechanisms are *not* considered for the design of the model. For the present study, the forward flight of the eagle helicopter was simulated to follow the desired trajectory. The servo input and sensor output data were collected and subsequently used for system identification. The state vector (x) and input vector (u) considered are,

$$\begin{aligned} x &= [\phi, \theta, \psi, u, v, w]^T; \\ u &= [\delta_{lon}, \delta_{lat}, \delta_{col}, \delta_{ped}]^T \end{aligned} \tag{15}$$

where [u, v, w] and [ϕ, θ, ϕ] represent body velocities and attitude vectors respectively, whereas [δ_{col}, δ_{ped}, δ_{lon}, δ_{lat}] represent the collective pitch, tail rotor pitch, longitudinal cyclic pitch and the lateral cyclic pitch, in that order.

2) Fixed-wing UAV model: The fixed-wing UAV data was simulated using the AeroSim blockset from Unmanned Dynamics© for the Aerosonde UAV. The AeroSim blockset is a Matlab® Simulink® toolbox that can be used for rapid development of 6-DOF aircraft dynamics [23]. The model was simulated with an elevator input (keeping throttle and rudder inputs as constants) applied to the 6-DOF AeroSim block. Sensor information from the gyroscopes, accelerometers and GPS were recorded for the purpose of estimation and system identification. The system dynamic equations used by the AeroSim blockset are standard 6-DOF equations and can be found in [6] and [17]. The state and input vectors used are,

$$\begin{aligned} x &= [\phi, \theta, \psi, u, v, w]^T \\ u &= [\delta_{ele}, \delta_{ail}, \delta_{thr}, \delta_{rud}]^T \end{aligned} \tag{16}$$

where [δ_{ele},δ_{ail},δ_{thr},δ_{rud}] represent the control surface deflections in elevator, aileron, throttle and rudder.

B. UKF-NN System Identification Results

The data for system identification was simulated with the following in mind:

- The sample time for data generation was set at 0.05sec as the fastest update rate available for commercial GPS is 20Hz.
- Both white noise and random bias were added to the simulated sensor data.

1) Rotary-wing System Identification: The proposed system identification described in Fig. 1 was applied to an Eagle rotary-wing UAV simulation model. The UKF was used for state estimation of attitude and body velocities ($\phi, \theta, \psi, u, v, w$) with gyro biases ($\varepsilon_p, \varepsilon_q, \varepsilon_r$). These states along with servo deflections were then provided as inputs to the NNID block for system identification. A maximum of two past values with one hidden layer and nine neurons were used for NNID. The control surface deflections ($\delta_{ped}, \delta_{lat}, \delta_{long}, \delta_{col}$) applied during the simulation process are as depicted in Fig. 2. The results from the state estimation and system identification for attitude and body-sensed

velocities are as illustrated in Fig. 3 and Fig. 4. The velocity estimation and system identification follow the system as shown in Fig. 4. A slight deviation from the system output is evident in case of pitch estimation (Fig. 3) as the pitch angle variation is very small when compared to the other angles.

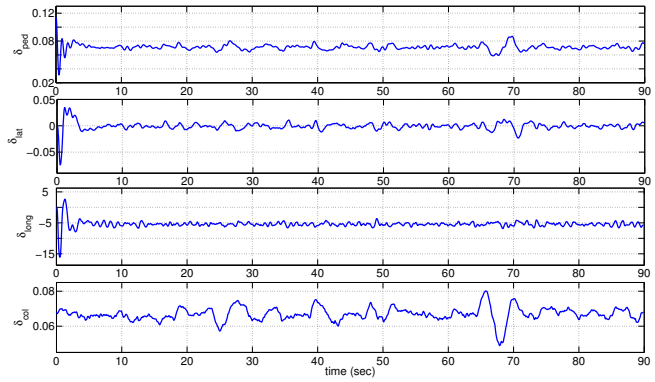

Fig. 2. Eagle Simulator: Control Surface Deflections

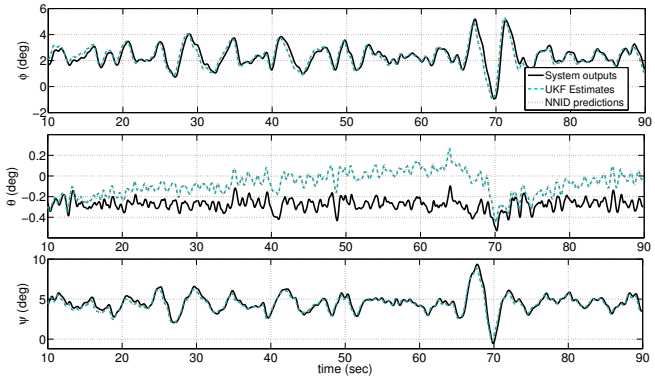

Fig. 3. NN Eagle System Identification: Attitude

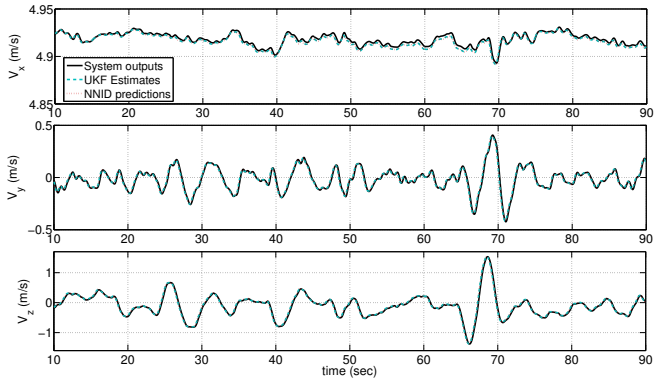

Fig. 4. NN Eagle System Identification: Velocities

A closer look into the statistical results in Table I suggests the proposed method to be suitable for estimation and identification of a 6-DOF Eagle model with acceptable error characteristics.

TABLE I
EAGLE SYSTEM ID STATISTICS: RMSE AND VARIANCE

Eagle ID Statistics		
	RMSE	Variance (1e-3)
ϕ	0.0256	0.3151
θ	0.0603	0.3477
ψ	0.0424	0.4902
u	0.0020	0.0001
v	0.0069	0.0001
w	0.0055	0.0007

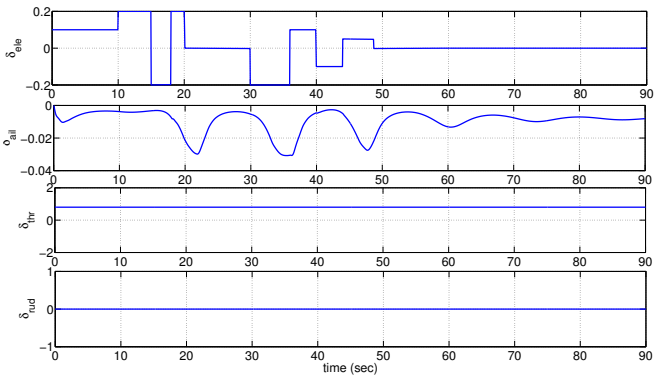

Fig. 5. Aerosonde Simulator: Control Surface Deflections

2) Fixed-wing System Identification: The Aerosonde model was tested for the system proposed in Fig. 1 for estimation and identification of attitude and body velocities $(\phi, \theta, \psi, u, v, w)$ with gyro biases $(\varepsilon_p, \varepsilon_q, \varepsilon_r)$. The predicted output from the ARX-NNID depend on the past and present inputs and outputs. A maximum of three past values were considered for calculations. The network architecture consist of a single hidden layer with a maximum of twelve neurons.

The control surface inputs $(\delta_{ele}, \delta_{ail}, \delta_{thr}, \delta_{rud})$ used to excite the dynamics are presented in Fig. 5. The corresponding attitude and body velocity estimation and system identification results are as illustrated in Fig. 6 and Fig. 7. The identification results and the error statistics from Table II might lead to a conclusion that the performance is degraded when compared to the rotary-wing model. However, this is attributed to the rapid elevator inputs as evident from Fig. 5, that are not generally used for a UAV with slow dynamics. Such an input sequence has been considered in order to account for extreme cases. Though there is a slight deviation from the estimated values, the NNID block does a good job of estimating the 6-DOF system with no signs of divergence.

VI. CONCLUSION AND FUTURE WORK

In this paper we have presented a novel UKF-NN framework for the system identification of a rotary-wing as well as a fixed-wing UAV. A UKF is used for reliable sensor fusion in order to provide high-quality sensor data to an NNID block for system identification. The rotary-wing Eagle simulation model was developed at UNSW@ADFA whereas the fixed-wing Aerosonde simulation model was adopted from the AeroSim blockset. The system identification results have

TABLE II

AEROSONDE SYSTEM ID STATISTICS: RMSE AND VARIANCE

Aerosonde ID Statistics		
	RMSE	Variance
ϕ	0.0903	0.0082
θ	0.1581	0.0250
ψ	0.3095	0.0958
u	0.0060	1e-5
v	0.0028	1e-5
w	0.0133	0.0001

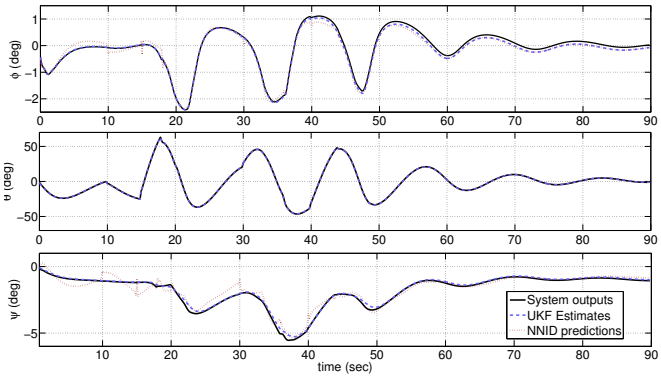

Fig. 6. NN Aerosonde System Identification: Attitude

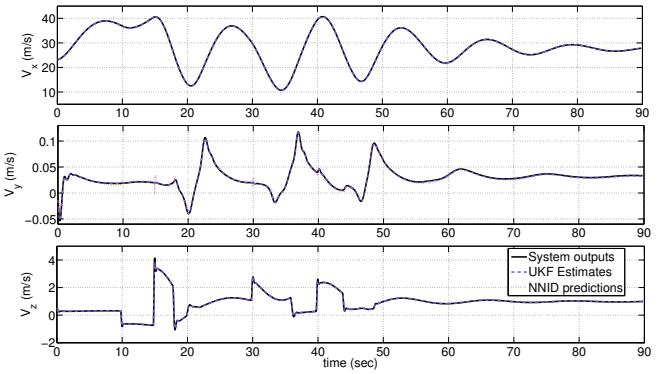

Fig. 7. NN Aerosonde System Identification: Velocities

been presented with error statistics and are shown to work for both UAV platforms with acceptable error characteristics.

Though a forward flight regime has been adopted for the UAVs, this might seldom be the case in real life, especially for rotary-wing UAVs. Our group is currently working on alternative attitude estimation methods to tackle this problem. Since the proposed UKF-NN identification framework seems to perform well for UAV simulation models, we are currently working on implementing the method in real-time.

REFERENCES

[1] A. J. Calise, E. N. Johnson, M. D. Johnson, and J. E. Corban, "Applications of adaptive neural-network control to unmanned aerial vehicles," in *AIAA/ICAS International Air and Space Symposium and Exposition: The Next 100 Years*. Dayton, OH: AIAA, 2003.

[2] V. Janardhan, D. Schmitz, and S. N. Balakrishnan, "Development and implementation of new nonlinear control concepts for a UA," in *23rd Digital Avionics Systems Conference*, vol. 2, 2004, pp. 12.E.5– 121–10.

[3] V. Puttige and S. Anavatti, "Real-time multi-network based identification with dynamic selection implemented for a low cost UAV," in *IEEE Conference on System, Man and Cybernetics*. Montreal, Canada: IEEE, 2007.

[4] M. K. Samal, S. Anavatti, and M. Garratt, "Neural network based system identification for autonomous flight of an eagle helicopter," in *The 17th IFAC World Congress*, Seoul, South Korea, July 2008.

[5] R. E. Kalman, "A new approach to linear filtering and prediction problems," *Transactions of the ASME–Journal of Basic Engineering*, vol. 82, no. Series D, pp. 35–45, 1960.

[6] J. A. Farrell and M. Barth, *The Global Positioning System & Inertial Navigation*, 1st ed. McGraw-Hill Professional, Dec. 1998.

[7] S. J. Julier and J. K. Uhlmann, "A new extension of the Kalman filter to nonlinear systems," in *Int. Symp. Aerospace/Defense Sensing, Simul. and Controls*, vol. 3, Orlando, FL, 1997.

[8] J. Kim, "Autonomous navigation for airborne applications," PhD Thesis, University of Sydney, 2004.

[9] D. B. Kingston and R. W. Beard, "Real-time attitude and position estimation for small UAVs using low-cost sensors," in *AIAA 3rd "Unmanned Unlimited" Technical Conference, Workshop and Exhibit*, Chicago, Illinois, 2004.

[10] D. Simon, *Optimal State Estimation: Kalman, H_∞, and Nonlinear Approaches*. Hoboken, New Jersey: Wiley-Interscience, 2006.

[11] R. van der Merwe, A. Doucet, N. de Freitas, and E. Wan, "The unscented particle filter," *Advances in Neural Information Processing Systems*, vol. 13, pp. 584–590, 2001.

[12] A. G. Kallapur, S. G. Anavatti, and M. A. Garratt, "Extended and unscented Kalman filters for attitude estimation of an unmanned aerial vehicle," in *27th IASTED International Conference on Modelling, Identification and Control (MIC)*. Innsbruck, Austria: ACTA Press, Feb. 2008.

[13] M. Napolitano, D. Windon, J. Casanova, M. Innocenti, and G. Silvestri, "Kalman filters and neural-network schemes for sensor validation in flight control systems," *Control Systems Technology, IEEE Transactions on*, vol. 6, no. 5, pp. 596–611, Sep 1998.

[14] F. Gao, F. Wang, and M. Li, "A neural-network-based nonlinear controller using an extended Kalman filter," *Industrial and Engineering Chemistry Research*, vol. 38, no. 6, pp. 2345–2349, 1999.

[15] J. de Jesús Rubio and W. Yu, "Nonlinear system identification with recurrent neural networks and dead-zone Kalman filter algorithm," *Neurocomput.*, vol. 70, no. 13-15, pp. 2460–2466, 2007.

[16] S. J. Julier, "The scaled unscented transformation," in *American Control Conference, 2002. Proceedings of the 2002*, vol. 6, 2002, pp. 4555–4559.

[17] B. Stevens and F. Lewis, *Aircraft Control and Simulation*, ser. Aircraft Control and Simulation. New York, USA: Wiley-Interscience, 1992.

[18] L. Ljung, *System Identification - Theory for the User*, 2nd ed. Prentice Hall, 1999.

[19] L. Ljung and J. Sjoberg, "A system identification perspective on neural networks," in *IEEE-SP Workshop Neural Networks for Signal Processing*. Helsingoer, Denmark: IEEE, Aug-Sep 1992, pp. 423–435.

[20] V. R. Puttige and S. G. Anavatti, "Real-time neural network based online identification technique for a UAV platform," in *International Conference on Computational Inteligence for Modelling Control Application*. Washington, DC, USA: IEEE Computer Society, 2006, p. 92.

[21] S. Haykin, *Neural Networks, A comprohensive foundation*. New York: Macmillan College Publishing Company, 1994.

[22] M. A. Garratt, "Biologically inspired vision and control for an autonomous flying vehicle," Ph.D. dissertation, The Australian National University, October 2007.

[23] Unmanned-Dynamics, "Aerosim aeronautical simulation blockset: user's guide," Hood River, OR, 2002. [Online]. Available: www.u-dynamics.com